Indian Journal of Pure & Applied Physics
Vol. 60, November 2022, pp. 909-913
DOI: 10.56042/ijpap.v60i11.65819

Structural, Dielectric and Electrical Properties of Homovalent Doped $SrSn_{1-x}Ti_xO_3$ ($0 \leq x \leq 0.08$) System

Aditya Kumar[a], Manoj K Singh[b], Minakshi Sharma[c] & Upendra Kumar[d*]

[a]Department of Physics, School of Science, IFTM University Moradabad-244 102, U.P. India
[b]Centre of Material Sciences, University of Allahabad, Prayagraj 211 002, India
[c]Department of Physical Sciences, Banasthali Vidyapith, Banasthali-304 022, Rajasthan India
[d]Advanced Functional Materials Laboratory, Department of Applied Sciences, IIIT Allahabad, Prayagraj, 211 015, India

Received: 23 August 2022; accepted 18 October 2022

The samples $SrSn_{1-x}Ti_xO_3$ with composition $0 \leq x \leq 0.08$ have been prepared using sol-gel chemical route by sintering at 1173 K. All the samples are found to be single phase crystallized in orthorhombic structure. The dielectric properties indicate the existence of interfacial and orientation polarization in samples found to be stable up to 300 °C. Thermal dependence of electrical conductivity represents two conduction regions with activation energy (0.77-0.94) eV in region-1 and (0.19-0.27) eV in region-2 respectively. The plot of dc conductivity with hopping frequency results unit slope representing that the charge carriers remain same in both processes. DC conductivity of samples are found to be increased with Ti^{4+}, due to reduction in polaron size. The present materials can be potentially used in thermally stable capacitor and mixed ionic and electronic conductors (MIECs) applications.

Keywords: $SrSn_{1-x}Ti_xO_3$; Sol-gel preparation; Electrical properties; Defects

1 Introduction

$SrSnO_3$ belongs to the perovskite family, characterized by general chemical formula ABO_3 with cations (A/B) and anion O. The modification made in $SrSnO_3$ either at Sr/Sn-site or both sites simultaneously tuned for various electronic devices, gas sensors, photocatalyst and transparent conducting oxide applications[1–3]. The modifications in $SrSnO_3$ can be done in two ways: (i) Homovalent (the dopant and host having same valency), (ii) Hetrovalent (the dopant has either higher or lower valency than host known as donor and acceptor respectively)[4]. Donor (M) type doping at Sr/Sn-site leads to an excess negative charge denoted as a positive defect ($M_{Sr}^{\cdot}, M_{Sn}^{\cdot}$) that would be compensated either by creating electron or cationic vacancy. Based on this modification, $SrSnO_3$ has been explored as proton conductor, gas sensor, and electrochemical devices *etc*.[5,6]. However, acceptor type (M) modification made at Sr/Sn-site leads an excess of positive charge denoted as negative defect ($M_{Sr}^{'}, M_{Sn}^{'}$) that would be compensated either by creating hole or oxygen vacancy[7]. Transition metal and rare earth modified (as acceptor) $SrSnO_3$ were explored as electrochemical devices, gas sensors, mixed ionic and electronic conductors (MIECs) in intermediate temperature solid oxide fuel cell (IT-SOFCs) applications[5,6,8,9]. Moreover, homovalent modified $SrSnO_3$ improved their dielectric properties due to generation of lattice strain[10]. Surprisingly, no detailed investigation on electrical properties of Ti^{4+} modified $SrSnO_3$ is still available in literature.

In present work, single phase $SrSn_{1-x}Ti_xO_3$ ($0 \leq x \leq 0.08$) was synthesized using sol-gel route by calcining at 1073 K and sintering at 1173 K for 10 h. The obtained powders were characterized using X-ray diffraction (XRD) to identify the phase of samples. The dielectric properties of silver coated pellets were recorded as a function of frequency (100 Hz to 100 KHz) within temperature range (25–530) °C.

2 Experimental

The samples of $SrSn_{1-x}Ti_xO_3$ (x=0, 0.02, 0.04, 0.06, 0.08) were synthesized using chemical route as described in elsewhere[10]. The phase of obtained samples was identified using Bruker D8 advance (U.S.A.) X-ray diffractometer employing Cu-Kα ($\lambda = 1.5418\,\text{Å}$) radiation. The electrical properties of silver coated pellets were studied using a high precision Alfa-A high-frequency Nova-Control impedance analyser as a function of frequency (100 Hz to 1 MHz) within temperature range (25–530) °C.

*Corresponding authors: (Email: upendra.bhu512@gmail.com)

3 Results and Discussions

In present investigation, the samples $SrSn_{1-x}Ti_xO_3$ with different doping concentration has been abbreviated as SSO. The samples with x=0.02, $SrSn_{0.98}Ti_{0.02}O_3$ has been referred as SSO2 and so on.

3.1 Structural Analysis

The phase identification of the samples is analysed using powder XRD analysis as shown in Fig S1. All the diffraction peaks observed in Fig S1 perfectly match to theoretical database (COD-1533387) reported for orthorhombic phase of $SrSnO_3$. However, the effect of dopant on the structural parameters is analyzed by Rietveld refinement performing on the XRD data. Fig. 1 (a-e) shows the refined pattern of all samples keeping the procedure similar to literature[10]. The parameters derived from refinement parameters are given in Table S1. The quality of fitting has been judged by calculating parameter S, and its value close to unity suggests parameters are relevant[11]. Substitution of Ti in the unit cell results compression of unit cell with Ti^{4+} due to its lower ionic radii (0.605 Å) than Sn^{4+} (0.69 Å). The calculation of crystallite size, micro-strain, and discussion of density explained in supplementary file. Crystal structure of reference sample shown in Fig. 1(f) revealed the presence of Sr at bcc, Sn at corner and oxygen at fcc, and with incorporation of Ti, it results compression in unit cell along all a, b, and c-direction.

3.2 Dielectric and Tangent Loss Analysis

The real part of dielectric constant (ε') and tangent loss ($\tan\delta$) with logarithmic frequency for a reference sample SSO4 are shown in Fig. 2 (a-b). The dielectric properties of ceramics are governed by different types polarization such as interfacial, ionic, orientational, and electronic those reacting in different frequency-range ranging from 1 mHz to several GHz[12]. The exponential rise observed in ε' and $\tan\delta$ plot at lower frequencies occurred due to interfacial polarization as well as higher response time[10]. The variation in both parameters (ε' and $\tan\delta$) above 10 KHz become lower due to orientational polarization effect. Since the samples are synthesized at higher temperature ~1173 K; so, possibility of oxygen loss cannot be excluded and given by;

$$O_o \rightarrow \frac{1}{2}O_2(g) + V_{\ddot{O}} + 2e' \quad \ldots (1)$$

The electron presents in above equation reduces the valence state of Sn (x=0) and Sn/Ti (x>0).

$$Sn^{4+} + 2e' \rightarrow Sn^{2+} \quad \ldots (2)$$

$$Ti^{4+} + e' \rightarrow Ti^{3+} + e' \rightarrow Ti^{2+} \quad \ldots (3)$$

Different dipoles like ${Sn^{2+}}_{Sn^{4+}}^{''} - V_{\ddot{O}}$, $2{Ti^{3+}}_{Ti^{4+}}^{'} - V_{\ddot{O}}$ and ${Ti^{2+}}_{Ti^{4+}}^{''} - V_{\ddot{O}}$ are formed in samples due to presence of these defects. The response time above 10 KHz results lower response time which is not sufficient for orientation of dipoles and gives lower ε' and $\tan\delta$. Therefore, the dopant's effect on ε' and $\tan\delta$ are analyzed at 10 KHz and shown in Fig. 2(c-d). Initially, ε' and $\tan\delta$ are found to be stable up 300 °C due to insufficient thermal

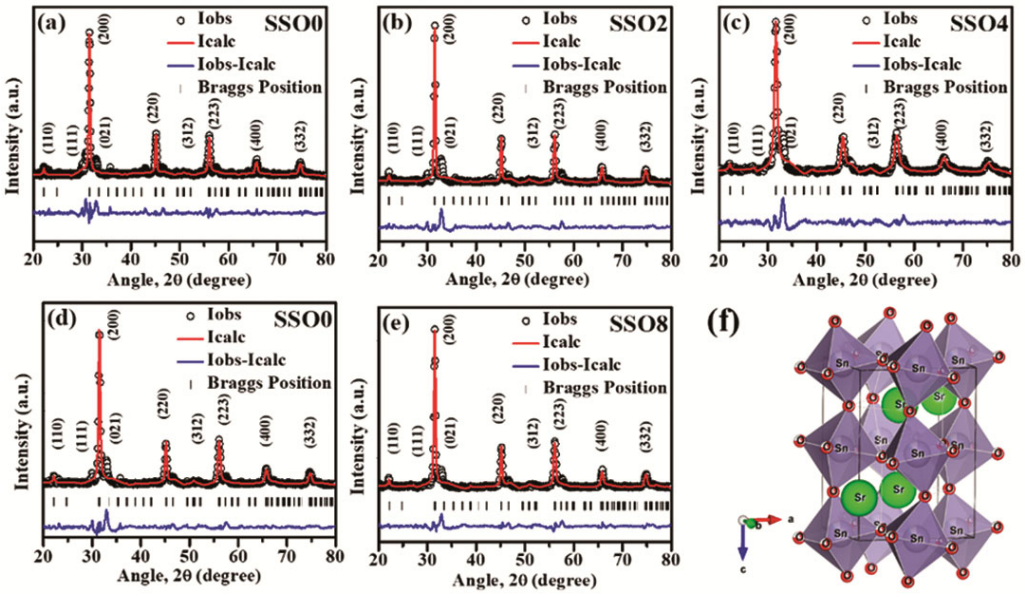

Fig. 1(a-e) — Rietveld refinement pattern of all samples, (f) Crystal structure of sample SSO4.

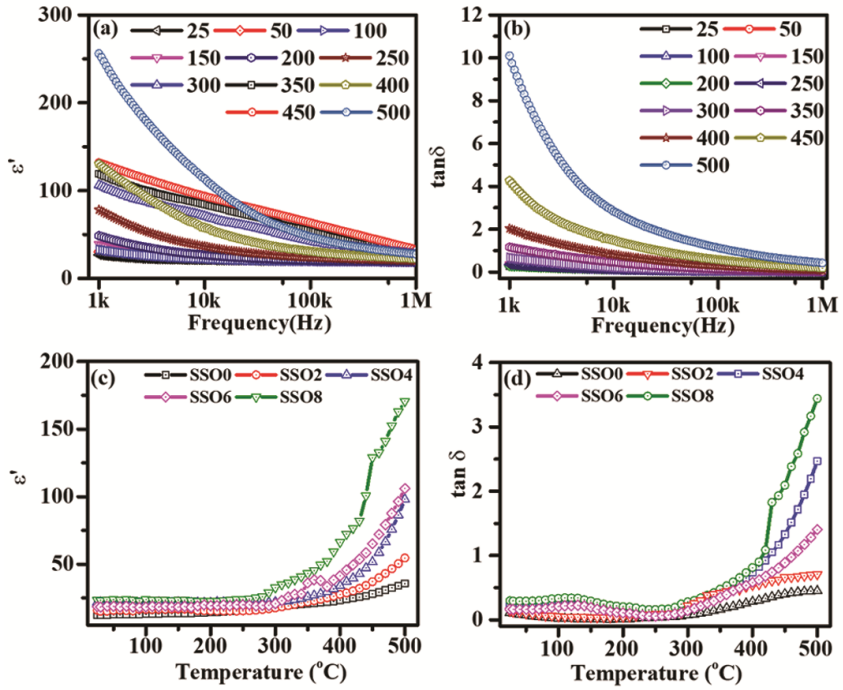

Fig. 2 — Frequency-dependence of (a) real part dielectric (b) tangent loss, for sample SSO4, Thermal-dependence of (c) real part dielectric (d) tangent loss, at 10 KHz for all samples.

energy while above 300 °C a linear rise is observed due to thermally activated process[12]. The behavior observed in samples makes it permissible candidate for thermally stable capacitor and sensor application.

3.3 Electrical Conductivity Analysis

To understand the thermal activated process involved in the sample, the ac conductivity of a reference sample is shown in Fig. 3(a). It depicts two regions: first region is frequency independent known as dc conductivity (σ_{dc}), and then linearly increases above crossover frequency known as hopping frequency (f_h) termed as ac conductivity (σ_{ac}). The total conductivity of electro-ceramics materials is given in terms of Jonscher's Power law[11];

$$\sigma = \sigma_{dc}\left(1 + \left(\frac{f}{f_h}\right)^n\right) \quad \ldots (4)$$

The value of σ_{dc}, f_h and power exponent (n) are extracted by fitting eq.(4) to experimental data of each sample at different temperatures. The logarithmic of σ_{dc} with inverse of temperature (1000/T) for all samples is displayed in Fig. 3(b). The Arrhenius model is used to investigate the conduction processes involved in samples and given by;

$$\log \sigma_{dc} = \log \sigma_0 + \left[-\frac{E_a}{1000*k}\left(\frac{1000}{T}\right)\right] \quad \ldots (5)$$

Where, σ_0 is pre-exponential factor, k is Boltzmann constant and E_a is the activation energy required for migration of charge carrier. The plot shows two conduction region with activation energy 0.78eV, 0.94eV, 0.77eV, 0.78eV, 0.87eV in region-1 and 0.26eV, 0.27eV, 0.19eV, 0.25eV and 0.24eV in region-2 from sample SSB0 to SSB8 respectively[11]. It has been further observed that the value of σ_{dc} found to be increased „with Ti, due to presence of defects such as $Sn^{2+}{}_{Sn^{4+}}$, $V_{\ddot{O}}$, and $Ti^{3+}{}_{Ti^{4+}}$; also supported by dielectric analysis. Further, to explore ac conduction process, the plot of $\log f_h$ with (1000/T) is shown in Fig. 3(c). It again shows similar conduction trend for all samples, and determined the activation energy by fitting 0.72eV, 0.80eV, 0.79eV, 0.72eV, and 0.76eV in region-1 and 0.15eV, 0.17eV, 0.16eV, 0.16eV, and 0.17eV in region-2 from SSB0 to SSB8 respectively. To elucidate the correlation between dc and ac conduction, both parameters are plotted against each other and depicts in Fig. 3(d) and found a straight line with slope almost unity. The unit slope of plot reflects that the charge carriers remain same in both ac and dc conduction process. The value of activation energy for region-1 is smaller than the region-2's activation energy. Activation energy for region-1 is consistent with polaronic conduction while region-2 is consistent with electronic conduction within ceramics, glasses, and glass-ceramics *etc.*[11]. The migration of polaron

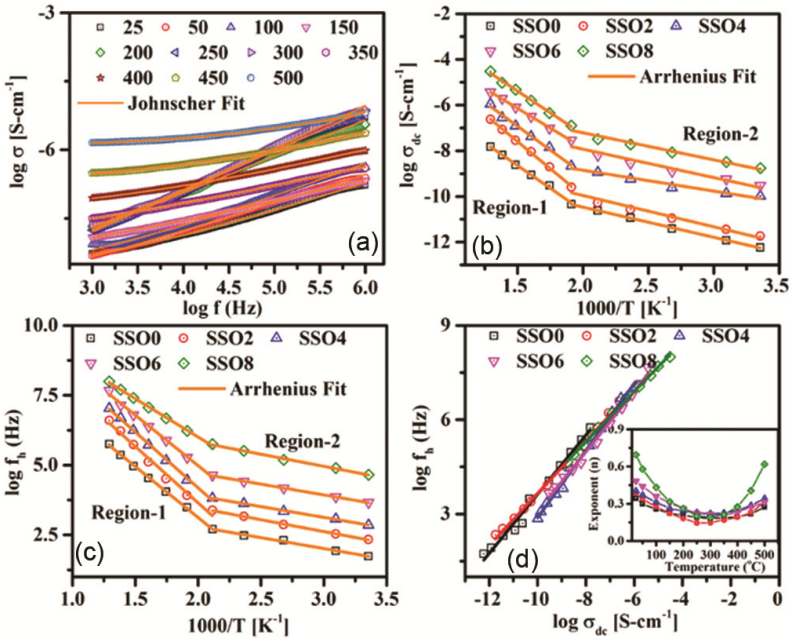

Fig. 3(a) — Frequency-dependent conductivity of sample SSO4 at different temperatures, Arrhenius plot generated from (b) dc conductivity (c) hopping frequency, (d) Variation of $\log \sigma_{dc}$ with $\log f_h$ (inset shows temperature dependance power exponent).

takes place via orientation of dipole ($Sn^{2+}{}_{Sn^{4+}}^{''} - V_{\ddot{O}}$, $2Ti^{3+}{}_{Ti^{4+}} - V_{\ddot{O}}$ and $Ti^{2+}{}_{Ti^{4+}} - V_{\ddot{O}}$) while electronic conduction takes place via hopping of electron between degenerates sites of Sn and Ti[13].

The power exponent has been used to explore conduction mechanism involved in ceramics[14]. So, the power exponent for all samples with temperature are shown in the inset of Fig 3(d). According to overlapping of large polaron tunneling model, initially n reduces to minimum value and then increased with temperature, which is consistent with present result. The size of polaron (L) is related to crystallite size (d) as $L \propto d^{1/3}$[(15 Ref)]. The L is calculated for each sample and given in Table S1, and found to decrease from 3.65 to 3.06 Å from sample SSB0 to SSB8 respectively. Value of L found to be higher than bond length Ti-O (Table S1) confirms the formation of large polaron.

4 Conclusions

Single phase samples of $SrSn_{1-x}Ti_xO_3$ ($x \leq 0.08$) were synthesized using sol-gel chemical route. All samples were crystallized into orthorhombic phase similar to $SrSnO_3$ and resulted gradual compression in unit cell with Ti due to its lower ionic radii. The frequency dependent ε' and $\tan\delta$ suggests the presence of interfacial and orientational polarization in sample, and it became constant with temperature (up to 300 °C) and increased linearly above 300 °C. DC conductivity of samples were increased with Ti substitution due to defects $Sn^{2+}{}_{Sn^{4+}}^{''}$, $V_{\ddot{O}}$, and $Ti^{3+}{}_{Ti^{4+}}^{'}$. Large over lapping polaron model accurately described the conduction process. The polaron size were decreased with Ti, further confirming the experimental findings. The present materials were considered for thermally stable capacitor and as MIECs in fuel cell application.

Acknowledgement

AK thankfully acknowledge the University Grant Commission (UGC), India for providing UGC research fellowship.

References

1 Shimizu Y, *J Electrochem* Soc, 136 (1989) 1206.
2 Hadjarab B, Bouguelia A & Trari M, *J Phys Chem Solids*, 68 (2007) 1491.
3 Liu Q, Dai J, Zhang X, Zhu G, Liu Z & Ding G, *Thin Solid Films*, 519 (2011) 6059.
4 Kumar U & Upadhyay S, *J Mater Sci Mater Electron*, 31 (2020) 5721.
5 Ishihara T, Fujita H, Nishiguchi H & Takita Y, *Sensors Actuators B Chem*, 65 (2000) 319.
6 Shah M A K Y, Zhu B, Rauf S, Mushtaq N, Yousaf M, Ali N, Tayyab Z, Akbar N, Yang C P & Wang B, *ACS Appl Energy Mater*, 3 (2020) 6323.
7 Kumar U & Upadhyay S, *Mater Res Express*, 6 (2019) 055805.
8 Thangadurai V, Beurmann P S & Weppner W, *Mater Sci Eng B Solid-State Mater Adv Technol*, 100 (2003) 18.
9 Azad A M, *J Electrochem Soc*, 139 (1992) 3690.

10 Kumar A, Khan B, Yadav V, Dixit A, Kumar U & Singh M K, *J Mater Sci Mater Electron, 31* (2020) 16838.
11 Kumar U & Upadhyay S, *Mater Lett*, 227 (2018) 100.
12 Kumar U, Ankur K, Yadav D & Upadhyay S, *Mater Charact*, 162 (2020) 110198.
13 Kumar A, Khan B, Singh G, Dixit A, Kumar U & Singh M K, *Phys Scr*, 95 (2020) 105807.
14 Kumar U & Upadhyay S, *J Electron Mater*, 48 (2019) 5279.
15 Suzuki T, Kosacki I, Anderson H U, Colomban P, Cnrs U M R & Pierre U, 14 (2007) 2007.